

# REPORT DOCUMENTATION PAGE

Form Approved  
OMB NO. 0704-0188

Public Reporting burden for this collection of information is estimated to average 1 hour per response, including the time for reviewing instructions, searching existing data sources, gathering and maintaining the data needed, and completing and reviewing the collection of information. Send comment regarding this burden estimates or any other aspect of this collection of information, including suggestions for reducing this burden, to Washington Headquarters Services, Directorate for Information Operations and Reports, 1215 Jefferson Davis Highway, Suite 1204, Arlington, VA 22202-4302, and to the Office of Management and Budget, Paperwork Reduction Project (0704-0188), Washington, DC 20503.

1. AGENCY USE ONLY (Leave Blank)		2. REPORT DATE 11/12/2003	3. REPORT TYPE AND DATES COVERED Final Progress Report, 07/12/1999 - 08/31/2003	
4. TITLE AND SUBTITLE Fabrication, Metrology and Modeling of Protective Coatings on Metallic MEMS Componets			5. FUNDING NUMBERS DAAD19-99-1-0283	
6. AUTHOR(S) Dr. Robert A. Weller				
7. PERFORMING ORGANIZATION NAME(S) AND ADDRESS(ES) Vanderbilt University, VU Station B #357749, Nashville, TN 37235-7749			8. PERFORMING ORGANIZATION REPORT NUMBER	
9. SPONSORING / MONITORING AGENCY NAME(S) AND ADDRESS(ES) U. S. Army Research Office P.O. Box 12211 Research Triangle Park, NC 27709-2211			10. SPONSORING / MONITORING AGENCY REPORT NUMBER  39512.9-MS	
11. SUPPLEMENTARY NOTES The views, opinions and/or findings contained in this report are those of the author(s) and should not be construed as an official Department of the Army position, policy or decision, unless so designated by other documentation.				
12 a. DISTRIBUTION / AVAILABILITY STATEMENT Approved for public release; distribution unlimited.			12 b. DISTRIBUTION CODE	
13. ABSTRACT (Maximum 200 words)  This project provided a proof-of-concept that indium tin oxide (ITO) thin films can be prepared on surfaces by pulsed laser deposition and configured as miniature strain gauges. The degree of piezoresistivity of the films is related to the oxygen content, with larger gauge factors correlated with oxygen excess. Typical gauge factors of order 10 were observed. Gauges as small as 20x100 microns were fabricated by focused ion beam milling and characterized. Radiation effects from ion beam milling were observed and measured. Structures encapsulated with silicon dioxide protective films retained their piezoresistive coefficient and were less susceptible to damage by focused ion beam imaging.				
14. SUBJECT TERMS indium tin oxide, ITO, strain gage, strain gauge, piezoresistivity, oxide semiconductor, thin film sensor			15. NUMBER OF PAGES 19	
			16. PRICE CODE	
17. SECURITY CLASSIFICATION OR REPORT UNCLASSIFIED	18. SECURITY CLASSIFICATION ON THIS PAGE UNCLASSIFIED	19. SECURITY CLASSIFICATION OF ABSTRACT UNCLASSIFIED	20. LIMITATION OF ABSTRACT UL	

NSN 7540-01-280-5500

Standard Form 298 (Rev. 2-89)  
Prescribed by ANSI Std. Z39-18  
298-102

Enclosure 1

**REPORT OF INVENTIONS AND SUBCONTRACTS**  
(Pursuant to "Patent Rights" Contract Clause) (See Instructions on back)

The public reporting burden for this collection of information is estimated to average 1 hour per response, including the time for reviewing instructions, searching existing data sources, gathering and maintaining the data needed, and completing and reviewing the collection of information. Send comments regarding this burden estimate or any other aspect of this collection of information, including suggestions for reducing the burden, to Department of Defense, Washington Headquarters Services, Directorate for Information Operations and Reports (9000-0095), 1215 Jefferson Davis Highway, Suite 1204, Arlington, VA 22202-4302. Respondents should be aware that notwithstanding any other provision of law, no person shall be subject to any penalty for failing to comply with a collection of information if it does not display a currently valid OMB control number.

**PLEASE DO NOT RETURN YOUR COMPLETED FORM TO THIS ADDRESS. RETURN COMPLETED FORM TO THE CONTRACTING OFFICER.**

1. a. NAME OF CONTRACTOR/SUBCONTRACTOR  
**Vanderbilt University**

c. CONTRACT NUMBER  
**DAAD19-99-1-0283**

2. a. NAME OF GOVERNMENT/PRIME CONTRACTOR  
**VU Station B #357749**

b. ADDRESS (Include ZIP Code)  
**Nashville, TN 37235-7749**

d. AWARD DATE (YYYYMMDD)  
**1999/07/12**

3. TYPE OF REPORT (X one)  
a. INTERIM  b. FINAL

4. REPORTING PERIOD (YYYYMMDD)  
a. FROM **1999/07/12**  
b. TO **2003/08/31**

**SECTION I - SUBJECT INVENTIONS**

5. "SUBJECT INVENTIONS" REQUIRED TO BE REPORTED BY CONTRACTOR/SUBCONTRACTOR ("None," so state)

NAME(S) OF INVENTOR(S) (Last, First, Middle Initial)	TITLE OF INVENTION(S)	DISCLOSURE NUMBER, PATENT APPLICATION SERIAL NUMBER OR PATENT NUMBER	ELECTION TO FILE PATENT APPLICATIONS (X)		CONFIRMATORY INSTRUMENT OR ASSIGNMENT FORWARDED TO CONTRACTING OFFICER (X)
			(1) UNITED STATES	(2) FOREIGN	
a. None			(a) YES <input type="checkbox"/>	(b) NO <input type="checkbox"/>	
b. None			(a) YES <input type="checkbox"/>	(b) NO <input type="checkbox"/>	
c. None			(a) YES <input type="checkbox"/>	(b) NO <input type="checkbox"/>	

g. ELECTED FOREIGN COUNTRIES IN WHICH A PATENT APPLICATION WILL BE FILED  
(1) TITLE OF INVENTION  
(2) FOREIGN COUNTRIES OF PATENT APPLICATION

**SECTION II - SUBCONTRACTS (Containing a "Patent Rights" clause)**

6. SUBCONTRACTS AWARDED BY CONTRACTOR/SUBCONTRACTOR ("None," so state)

NAME OF SUBCONTRACTOR(S)	ADDRESS (Include ZIP Code)	SUBCONTRACT NUMBER(S)	FAR "PATENT RIGHTS"		DESCRIPTION OF WORK TO BE PERFORMED UNDER SUBCONTRACT(S)	SUBCONTRACT DATES (YYYYMMDD)	
			(1) CLAUSE NUMBER	(2) DATE (YYMM)		(1) AWARD	(2) ESTIMATED COMPLETION
a. None							


**SECTION III - CERTIFICATION**

7. CERTIFICATION OF REPORT BY CONTRACTOR/SUBCONTRACTOR (of required if (X as appropriate))  
SMALL BUSINESS OR  NONPROFIT ORGANIZATION

I certify that the reporting party has procedures for prompt identification and timely disclosure of "Subject Inventions," that such procedures have been followed and that all "Subject Inventions" have been reported.

a. NAME OF AUTHORIZED CONTRACTOR/SUBCONTRACTOR OFFICIAL (Last, First, Middle Initial)  
**John T. Childress**

b. TITLE  
**Director, Division of Sponsored Research**

c. SIGNATURE  


d. DATE SIGNED  
**9.13.03**

# Fabrication, Metrology and Modeling of Protective Coatings on Metallic MEMS Components

## Final Report

Robert A. Weller

November 7, 2003

U. S. Army Research Office

DAAD 19-99-1-0283

VANDERBILT UNIVERSITY

NASHVILLE, TENNESSEE

Approved for Public Release;

Distribution Unlimited.

THE VIEWS, OPINIONS, AND FINDINGS CONTAINED IN THIS REPORT ARE THOSE OF THE AUTHOR AND SHOULD NOT BE CONSTRUED AS AN OFFICIAL DEPARTMENT OF THE ARMY POSITION, POLICY, OR DECISION, UNLESS SO DESIGNATED BY OTHER DOCUMENTATION.

## STATEMENT OF THE PROBLEM

The original motivation for this work was to develop coating for metallic MEMS components to improve their performance and reliability. During a review of refractory oxides a report came to our attention that indium tin oxide (ITO), well known as the most widely used transparent conductor, is also piezoresistive. Thus, in principle, coating of ITO either alone or in combination with other thin films might be both protective and electrically functional.

The thrust of this project has been to deposit and test pulsed laser deposited thin films of ITO to confirm and optimize piezoresistivity as a function of film properties and formation conditions. Test structures were fabricated in a form similar to practical gauges and gauge factors were used to characterize the materials. Films were measured as deposited on glass substrates and with protective  $\text{SiO}_2$  layers over them. The electrical response was determined as a function of oxygen content and following particle radiation.

This report summarizes the results of the project and other relevant information.

## SUMMARY OF IMPORTANT RESULTS

This project has provided a proof-of-concept that indium tin oxide (ITO) thin films can be deposited on surfaces and configured as miniature strain gauges. Arguably, the most important observation has been that the piezoresistivity of ITO is related to the oxygen content and that samples with the largest piezoresistivity as determined by measured gauge factor are those with the largest excess of oxygen. This property distinguishes piezoresistive ITO films from those that optimize conductivity and transparency. It is essential to note that insofar as this work is concerned the transparent-conductor behavior of ITO is irrelevant. Rather, this work deals with another interesting property of this already interesting oxide semiconductor, the conductivity as a function of mechanical deformation. Data available at the time of the completion of the project are consistent with a model for the piezoresistive effect analogous to that often employed to describe hopping conduction in amorphous materials. This idea appears in preliminary form in the thesis by Hui Fang cited in the publication list below and is being developed for future publication. Many of the important experimental details and techniques are described in the papers by Miller et al., citation 1 and Fang et al. citation 3 in section (a) of the publication list that follows. These papers are included in the Appendix to supplement this brief summary.

## PUBLICATIONS

### (A) REVIEWED PUBLICATIONS

1. T. M. Miller, H. Fang, R. H. Magruder and R. A. Weller, "Fabrication of a micro-scale indium tin oxide thin film strain sensor by pulsed laser deposition and focused ion beam machining," *Sensors and Actuators A*, vol. 104, pp. 162-170, 2003.
2. R. A. Weller, W. T. Ryle, A. T. Newton, M. D. McMahon, T. M. Miller, and R. H. Magruder, III, "A Technique for Producing Ordered Arrays of Metallic Nanoclusters by Electroless Deposition in Focused Ion Beam Patterns," *IEEE Transactions on Nanotechnology*, vol. 2 pp. 154-157, 2003. (Undergraduate students funded by ARO worked on this project.)
3. H. Fang, T. M. Miller, R. H. Magruder, III, and R. A. Weller, "The effect of strain on the resistivity of indium tin oxide films prepared by pulsed laser deposition," *Journal of Applied Physics*, vol. 91, pp. 6194-96, 2002.
4. K. Telari, B. Rogers, H. Fang, L. Shen, R. A. Weller and D. N. Braski, "Characterization of platinum films deposited by focused ion beam-assisted chemical vapor deposition," *Journal of Vacuum Science and Technology B*, vol. 20, pp. 590-595, 2002.

5. T. S. Fisher, D. G. Walker, R. A. Weller, "Analysis and simulation of anode heating from electron field emission," Eighth Intersociety Conference on Thermal and Thermomechanical Phenomena in Electronic Systems, San Diego, June 2002. *IEEE Transactions on Components and Packaging Technologies*, vol. 26, No. 2, pp. 317-323, 2003. (This paper, a theoretical work involving thin films and nanostructures, used computational capability developed with ARO support.)
6. R. A. Weller, "An algorithm for computing linear four-point probe thickness correction factors," *Review of Scientific Instruments*, vol. 72, pp. 3580-3586, 2001.

(B) PUBLISHED IN CONFERENCE PROCEEDINGS

1. R. F. Haglund, Jr., R. A. Weller, C. E. Heiner<sup>1</sup>, M. D. McMahon, R. H. Magruder, III, A. T. Newton, L. Shen and L. C. Feldman, "Fabricating Two-Dimensional Metal Nanocrystal Arrays Using Pulsed-Laser Deposition and Focused Ion-Beam Technologies," *Materials Research Society Symposium Proceedings*, vol. 636, pp. D5.6.1-D5.6.6, 2001. (The FIB work discussed in this paper was done in part in support of the sensor work discussed in this report.)

(C) PRESENTED AT MEETINGS (ALL INVITED)

1. R. A. Weller, "Toward a comprehensive quantitative workbench for surface analysis," Seventeenth International Conference on the Application of Accelerators in Research and Industry, University of North Texas, Denton, Texas, November 12-16, 2002. (Host, J. Tesmer, Los Alamos National Laboratory)
2. R. A. Weller, "Toward a comprehensive quantitative workbench for surface analysis," 49<sup>th</sup> International Symposium, American Vacuum Society, Denver, Colorado, November 3-8, 2002. (Session Chair, C. R. Brundle, Applied Materials)
3. R. A. Weller, "Time of flight medium energy backscattering," Surface Analysis, 2002, American Vacuum Society, Nashville, Tennessee, May 20-22, 2002. (Session Chair, N. Winograd, Pennsylvania State University)
4. R. A. Weller, "Development of techniques for direct deposition of microsensors for MEMS applications," presented at the Workshop on Microsystems Technology and Applications, U. S. Army Aviation and Missile Command, Redstone Arsenal, Alabama, July 11-12, 2001.

5. R. A. Weller, "High resolution medium energy ion beam analysis of ultra-thin oxides," TMS Fall Meeting, Indianapolis, Indiana, November 4-8, 2001. (Given at the Symposium honoring R. R. Reeber of ARO.)
6. R. A. Weller, "Development of techniques for direct deposition of microsensors for MEMS applications," Microsystems Technology and Applications Workshop, Redstone Arsenal, July 11-12, 2001.
7. R. A. Weller, "Laser deposition and ion beam fabrication for MEMS applications," NASA/AMCOM joint MEMS working group at the Redstone Arsenal on 24 March 2000.

#### (D) BOOK CHAPTERS AND THESES

1. Hui Fang, "Piezoresistivity of indium tin oxide thin films prepared by pulsed laser deposition," Ph.D. Thesis, Vanderbilt University, August, 2003.
2. Timothy M. Miller, "Fabrication of a micro-scale indium-tin-oxide thin film strain sensor by pulsed laser deposition and focused ion beam machining for micro-machines," M.S. Thesis, Vanderbilt University, December, 2002.
3. R. A. Weller, "Introduction to Medium Energy Ion Beam Analysis," Unit 12b in **Methods in Materials Research**," John Wiley & Sons, Inc., New York, 2000, pp. 12b.1-12.2.
4. R. A. Weller, "Medium-Energy Backscattering and Forward-Recoil Spectrometry," Unit 12b.1 in **Methods in Materials Research**, John Wiley & Sons, Inc., New York, 2000, pp. 12b1.1-12b.1.15.

## PARTICIPATING SCIENTIFIC PERSONNEL

Here we list those persons who participated at a substantial level in bringing this facility on line and who are continuing to perform computations with it. The students are doing work similar to our original proposal but in conjunction with an unrelated program sponsored by the Navy.

- Robert A. Weller, Vanderbilt University. Principal investigator.
- Robert H. Magruder, III, Vanderbilt University and Belmont University. Co-Principal investigator.
- Michael Goldfarb, Vanderbilt University. Consulting senior investigator. Co-advisor of T. Miller's M.S. thesis.

- Bridget R. Rogers, Vanderbilt University. Consulting senior investigator.
- Hui Fang. Graduate student. Fang earned a Ph.D. degree through participation in this project.
- Timothy M. Miller. Graduate student. Miller earned an M.S. degree through participation in this project.
- Wesley T. Ryle. Summer undergraduate research student.
- Allan T. Newton. Summer undergraduate research student.
- Matthew D. McMahon. Summer undergraduate research student, and subsequently graduate student, Dept. of Physics, Vanderbilt.

## REPORT OF INVENTIONS

B. L. Doyle, G. Vitzkelethy, and R. A. Weller, Ion-induced electron emission microscopy, U. S. Patent number 6,291,823, September 18, 2001.



## APPENDIX

This appendix includes reprints of two papers that describe most of the substantial findings of this research project. The most complete description of the experimental details is the M.S. Thesis of Miller cited in the publication list above. The Ph.D. thesis of Fang has the most detailed description of the basic physics and our current thoughts about possible mechanisms.

1. "The effect of strain on the resistivity of indium tin oxide films prepared by pulsed laser deposition," H. Fang, T. M. Miller, R. H. Magruder, III, and R. A. Weller, *Journal of Applied Physics*, vol. 91, pp. 6194-96, 2002.
2. "Fabrication of a micro-scale indium tin oxide thin film strain sensor by pulsed laser deposition and focused ion beam machining," T. M. Miller, H. Fang, R. H. Magruder and R. A. Weller, *Sensors and Actuators A*, vol. 104, pp. 162-170, 2003.

# The effect of strain on the resistivity of indium tin oxide films prepared by pulsed laser deposition

Hui Fang

*Department of Physics and Astronomy, Vanderbilt University, Nashville, Tennessee 37235*

Timothy M. Miller

*Department of Mechanical Engineering, Vanderbilt University, Tennessee 37235*

Robert H. Magruder, III

*Department of Physics, Belmont University, Nashville, Tennessee 37212 and Department of Electrical Engineering and Computer Science, Vanderbilt University, Nashville, Tennessee 37235*

Robert A. Weller<sup>a)</sup>

*Department of Electrical Engineering and Computer Science and Department of Physics and Astronomy, Vanderbilt University, Nashville, Tennessee 37235*

(Received 29 November 2001; accepted for publication 5 February 2002)

The piezoresistivity of thin films of indium tin oxide prepared by pulsed laser deposition has been measured as a function of processing parameters. The thickness of the films ranged from 200 to 1200 nm. Resistivity and strain sensitivity measurements as a function of laser deposition parameters are reported. Gauge factors, defined as the ratio of the fractional resistance change to the applied strain, were observed to vary from approximately 0.2 for deposition in vacuum to as large as  $-14.7$  for deposition with a residual atmosphere of 50 mTorr of oxygen. The response of gauges to strains up to the measurement limit of approximately  $220 \mu\epsilon$  was both linear and free of hysteresis. This fabrication strategy makes possible the direct deposition of sub-mm strain gauges onto surfaces and components, including those of micro electromechanical systems. © 2002 American Institute of Physics. [DOI: 10.1063/1.1465115]

Indium tin oxide (ITO) is known primarily as a transparent conductor and is the most widely used material with this unusual property.<sup>1</sup> ITO is almost always used as a thin film and has been prepared in this form by evaporation, spray pyrolysis, magnetron sputtering, chemical vapor deposition, and pulsed laser deposition.<sup>2</sup> It is an *n*-type, degenerately doped, wide band gap semiconductor whose plasma frequency is just below the visible range of the spectrum and whose interband absorption edge is just above it. Charge carriers are thought to be provided both by tin atoms in indium sites acting as donors and by free electrons from oxygen vacancies. ITO has also been reported to exhibit a piezoresistive response comparable to *p*-type, single-crystal Si making it a promising material for microscale, directly deposited strain sensors.<sup>3,4</sup>

Directly deposited thin film strain gauges offer important advantages over conventional gauges, including unobtrusive operation, negligible mass and profile, low current operation, and the potential for production in complex configurations with little added effort. In addition, the full range of processes and techniques of thin film science can be brought to bear for both manufacture and characterization of the resulting devices. Thus, structures can be tailored for specific applications, including, for example, layers for electrical or thermal insulation, while avoiding complex assembly steps involving delicate parts placement and adhesive application.

The responsiveness of a strain sensor is parameterized by a quantity called the gauge factor,  $g$ , defined in Eq. (1) as the fractional resistance change per unit strain. In this equation,  $R$  is the initial resistance of the gauge structure and  $\Delta R$  is the change in resistance accompanying a strain  $\epsilon$ :

$$g \equiv \frac{\Delta R}{R} \frac{1}{\epsilon}. \quad (1)$$

For semiconductor gauges, it is useful to elaborate upon Eq. (1) by separating the dependence of  $R$  on the geometry of the gauge and resistivity  $\rho$  of the material used to make it. The result of this separation is Eq. (2), where Poisson's ratio  $\nu$  quantifies the contribution of geometric deformation to resistance change, and the effect the variation in intrinsic resistivity  $\Delta\rho/\rho$  is expressed explicitly:

$$g = 1 + 2\nu + \frac{\Delta\rho}{\rho} \frac{1}{\epsilon}. \quad (2)$$

The extrinsic geometric effects parameterized by  $\nu$  dominate in metal foil strain gauges. In semiconductor gauges, geometric effects are minimal and are often ignored. The variability of intrinsic resistivity with mechanical stress in an elastically strained material is called piezoresistivity.<sup>5</sup> The origin of piezoresistivity in crystalline semiconductors such as Ge and Si has been discussed by various authors.<sup>6</sup> However, the structure of ITO is sufficiently different that direct comparisons with earlier theory are problematic.

Gauge factors as large as  $-77$  have been reported for ITO.<sup>3</sup> By comparison, the gauge factors of semiconductor

<sup>a)</sup>Electronic mail: robert.a.weller@vanderbilt.edu

silicon gauges are typically in the range  $-20$  to  $-120$ ,<sup>7</sup> while those of metal foil gauges are positive and less than about 6.<sup>8</sup> Previous research on ITO's strain sensing properties has involved films deposited by magnetron sputtering. In the work reported here, all films have been produced by pulsed laser deposition, because of the greater control that can be exercised over the film's stoichiometry,<sup>2,9</sup> and because, in analogy to the situation in glass,<sup>10</sup> the properties of ITO may be more strongly influenced by the mode of formation than those of conventional crystalline semiconductors.<sup>11</sup>

Thin films of ITO were prepared by pulsed laser deposition (PLD) using commercial pressed-powder laser targets of 90%  $\text{In}_2\text{O}_3$  and 10%  $\text{SnO}_2$  obtained from Kurt J. Lesker, Co. A krypton-fluoride excimer laser (Lambda Physik Compex 205) producing 248 nm pulses with a fluence of  $\sim 3 \text{ J/cm}^2/\text{pulse}$  was used to ablate the target. The repetition rate of the laser was 10 Hz and the number of laser pulses was selected to produce films with uniform thicknesses ranging from  $\sim 200$  to  $\sim 1200$  nm.

The ITO films were deposited on substrates of Corning glass 2935 with dimensions of  $50 \text{ mm} \times 24 \text{ mm} \times 0.16 \text{ mm}$ . Prior to deposition, each glass slide was cleaned in a series of sonic baths of acetone, methanol, and distilled water, and then blown dry with compressed dry  $\text{N}_2$ . The substrates were positioned behind a shadow mask on a rotating, temperature-controlled stage 6 cm above the target. The shadow mask produced a consistently dimensioned structure for measurements approximately  $1 \text{ mm} \times 5 \text{ mm}$ , in a conventional four-point probe configuration, as well as uniform pads for electrical contacts. These contacts were made using  $25\text{-}\mu\text{m}$ -thick gold wires and a conductive epoxy (H20E from Epotek Corporation) that adheres well to both ITO and gold.

Prior to all depositions the chamber was evacuated to a base pressure of approximately  $10^{-6}$  Torr. Depositions were then performed with varying substrate temperatures from ambient to  $200^\circ\text{C}$  and with oxygen partial pressures from base pressure to 50 mTorr. The oxygen partial pressure was controlled with a mass flow controller and throttle valve using 99.999% pure oxygen. A Dektak II stylus profilometer was used to measure film thickness.

The gauge factor was measured using a four-point-bending apparatus excited by a precision constant current source (HP-E3631A). The apparatus was calibrated with a commercial metal foil strain gauge. In order to maximize the electrical signal to noise ratio, the apparatus was fully shielded within a Faraday cage. Four-point electrical resistance measurements were made using a Keithley 236 constant current source for excitation and a Keithley 2001 7 1/2 digit multimeter for the voltage measurement.

The oxygen partial pressure during laser deposition has been shown previously to be a crucial parameter determining the resistivity of ITO films.<sup>2,9</sup> Oxygen vacancies contribute charge carriers and as a result, varying the oxygen stoichiometry through  $\text{O}_2$  background pressure during deposition is in effect a means for controlling carrier density. Consequently, the effect of the pressure of  $\text{O}_2$  on the strain sensitivity of the resistivity is of significant interest. Figure 1 shows curves of the resistivity and gauge factor of ITO as a function of  $\text{O}_2$  ambient pressure during deposition. Resistiv-

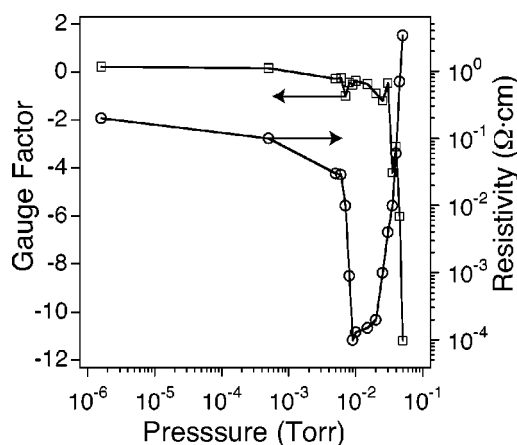


FIG. 1. Variation of gauge factor and resistivity with oxygen partial pressure for ITO films deposited by PLD. The gauge factor is shown by open squares, the resistivity by open circles.

ity is given in units of  $\Omega \text{ cm}$  and is plotted on the right axis. The gauge factor, a pure number, is plotted on the left axis. The most significant conclusion to be drawn from Fig. 1 is that the condition for lowest resistivity of the deposited film differs significantly from the condition for optimum piezoresistivity.

For the lowest deposition pressures around  $10^{-6}$  Torr, samples exhibited an essentially metallic behavior with the gauge factor being small and positive. Under conditions for optimum resistivity, around 9 mTorr where the resistivity is  $\sim 10^{-4} \Omega \text{ cm}$ , the gauge factor of the material was only about  $-0.52$ . At the highest pressure achievable in our system, 50 mTorr, the resistivity was  $3.4 \Omega \text{ cm}$ , while the average gauge factor of similarly prepared samples was  $-11 \pm 3$ . The (signed) value of the gauge factor decreased monotonically with increasing background pressure of oxygen in the range observed. The estimated error in the measured gauge factor is less than 20% when the absolute value of the gauge factor is less than unity, approximately 10% for gauge factors between 1 and 4, and 5% for those between 4 and 12.

Figure 2 shows the change in resistance as a function of applied strain for a typical gauge structure prepared with an

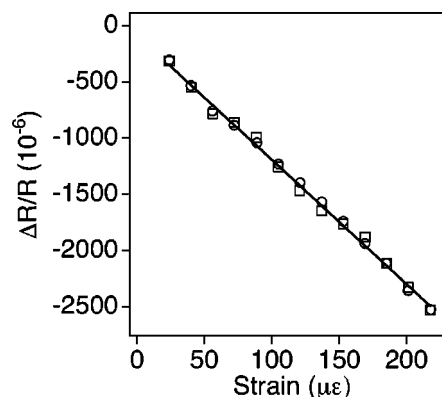


FIG. 2. Resistance change with strain of an ITO film deposited with oxygen ambient pressure of 50 mTorr. The thickness of the film is 564 nm. Open circles are data taken with increasing strain, open squares were taken with decreasing strain.

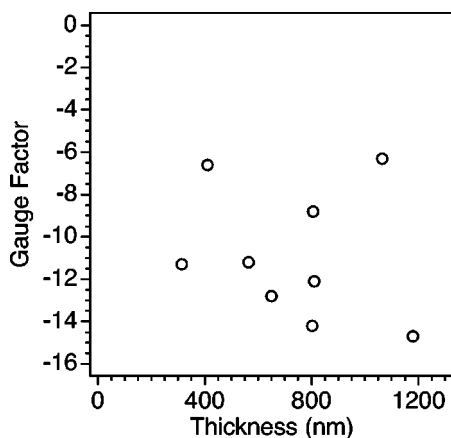


FIG. 3. The gauge factor as a function of film thickness for oxygen ambient pressure of 50 mTorr.

oxygen partial pressure of 50 mTorr. The example shown has a gauge factor of  $-11.2$ . The measurement errors for each point in Fig. 3 are less than 2% and are therefore not shown explicitly. This graph contains points measured during both increasing and decreasing strain conditions and thus demonstrates an absence of hysteresis that was typical of the films measured in this work.

The thickness of films prepared by PLD has been reported to affect the crystallinity and grain size, with thicker samples reported to be more crystalline and to have larger grain size.<sup>2</sup> Since these parameters may have a significant impact on the piezoresistivity of ITO, the gauge factors of nine samples with thickness ranging from 260 to 1200 nm were measured. Samples were made at room temperature and at an oxygen partial pressure, 50 mTorr. Figure 3 shows the gauge factor for these samples as a function of sample thickness. There is no apparent correlation between gauge factor and the sample thickness for the range of thicknesses studied. The large scatter in these data is attributed, at least in part, to the difficulty in controlling the system pressure to high accuracy in a region in which the gauge factor is a sensitive function of pressure (see Fig. 1). We conclude that for the range of thicknesses reported here the gauge factor is not a strong function of film thickness.

Temperature stability is an essential characteristic if ITO is to be used in high temperature strain gauges. Previous work has shown significant changes in the gauge factor for

ITO thin films prepared by rf sputtering when annealed in nitrogen.<sup>3</sup> In our work, samples were annealed at 450 °C in 99.999% nitrogen for 1 h with no significant effect on the gauge factor observed to result from this treatment. This difference relative to the results of Dyer *et al.*<sup>3</sup> may be due to differences in the mode of formation between laser and sputter deposited films. The properties of ITO are known to depend strongly on the mode of formation.<sup>11</sup> We conclude from this result that the PLD process produces very stable films that are not significantly changed by annealing under the conditions reported here.

In conclusion, laser deposited indium tin oxide films have been observed to exhibit a stable, hysteresis-free piezoresistive response with gauge factors as large as approximately  $-15$ . Gauge factors were largest in absolute value when the films were deposited at room temperature in the highest achievable background pressure of  $O_2$ , although these films exhibited moderately large sample-to-sample variability, suggesting that an important processing parameter may be as yet unidentified. Annealing in a nitrogen atmosphere produced no significant change in piezoresistive response. The observed properties of this material make it a strong candidate for direct deposition of strain sensors on microsystem components and other surfaces where semiconductor silicon gauges are impractical.

#### ACKNOWLEDGMENTS

This work was supported by the U.S. Army Research Office under grant DAAD 19-99-1-0283 and by NASA under Grant No. NGT8-52905.

- <sup>1</sup>B. G. Lewis and D. C. Paine, *MRS Bull.* **25**, 22 (2000).
- <sup>2</sup>H. Kim, C. M. Gilmore, A. Piqué, J. S. Horwitz, H. Matsoussi, H. Murata, Z. H. Kafafi, and D. B. Chrisey, *J. Appl. Phys.* **86**, 6451 (1999).
- <sup>3</sup>S. E. Dyer, O. J. Gregory, P. S. Amons, and A. B. Slot, *Thin Solid Films* **288**, 279 (1996).
- <sup>4</sup>O. J. Gregory and Q. Luo, *Sens. Actuators A* **88**, 234 (2001).
- <sup>5</sup>C. S. Smith, *Phys. Rev.* **94**, 42 (1954) and references therein.
- <sup>6</sup>P. Kleimann, B. Semmache, M. Le Berre, and D. Barbier, *Phys. Rev. B* **57**, 8966 (1998) and references therein.
- <sup>7</sup>V. Mosser, J. Suski, J. Gross, and E. Obermeier, *Sens. Actuators A* **28**, 113 (1991).
- <sup>8</sup>W. M. Murray and W. R. Miller, *The Bonded Electrical Resistance Strain Gauge* (Oxford University Press, New York, 1992), pp. 13, 39.
- <sup>9</sup>Y. Wu, C. H. M. Marée, R. F. Haglund, Jr., J. D. Hamilton, M. A. Morales Paliza, and R. A. Weller, *J. Appl. Phys.* **86**, 991 (1999).
- <sup>10</sup>D. Turnbull, *Diffusion and Defect Data* **53–54**, 9 (1987).
- <sup>11</sup>R. B. H. Tahar, T. Ban, Y. Ohya, and Y. Takahashi, *J. Appl. Phys.* **83**, 2631 (1998).

# Fabrication of a micro-scale, indium-tin-oxide thin film strain-sensor by pulsed laser deposition and focused ion beam machining

Timothy M. Miller<sup>a</sup>, Hui Fang<sup>b</sup>, Robert H. Magruder III<sup>c,d</sup>, Robert A. Weller<sup>b,d,\*</sup>

<sup>a</sup>Department of Mechanical Engineering, Vanderbilt University, Nashville, TN 37235, USA

<sup>b</sup>Department of Physics and Astronomy, Vanderbilt University, Nashville, TN 37235, USA

<sup>c</sup>Department of Physics, Belmont University, Nashville, TN 37212, USA

<sup>d</sup>Department of Electrical Engineering and Computer Science, Vanderbilt University, P.O. Box 1824 Station B, Nashville, TN 37235, USA

Received 1 October 2002; received in revised form 15 January 2003; accepted 19 January 2003

## Abstract

A thin film strain-sensor having an active sensing area of 20 mm × 100 mm has been developed using a combination of pulsed laser deposition (PLD) and focused ion beam (FIB) machining to net shape. Sensors were made of indium-tin-oxide (ITO) thin films in the range 100–246 nm thick. Strain sensitivities of large-scale (smallest dimension = 0.8 mm), small-scale (smallest dimension = 0.25 mm) and FIB machined gages (smallest dimension = 20 μm) are reported. Large-scale devices were deposited in a background oxygen pressure in the range 28–50 mTorr, while small-scale and FIB machined gages were deposited in 50 mTorr of oxygen, the largest achievable pressure in our system, which also yielded the largest strain sensitivities. Active strain-sensors were produced with gage factors ranging from −0.3 to −8.7 and showed a linear room temperature response with minimal hysteresis. The effects of imaging and machining with the FIB as well as the effects of an SiO<sub>2</sub> encapsulation layer on the electrical properties of the gages are reported.

© 2003 Elsevier Science B.V. All rights reserved.

**Keywords:** Thin film; Strain-sensor; Indium-tin-oxide; Pulsed laser deposition; Focused ion beam; MEMS

## 1. Introduction

Goldfarb and Celanovic have described a flexure-based gripper for micromanipulation [1]. For a tool such as this, designed to handle objects in the size range from 5 to 100 μm, monitoring the gripping force is a necessity. A technology that adds sensing capabilities to micro-scale systems will have to surpass the limitations of conventional strain gages. One possibility uses direct deposition of a sensing material and has the advantage of avoiding adhesives and manual manipulation. Subsequent micro-machining of gage structures has the advantage of tailoring a sensor for a specific application. The addition of tactile feedback by the integration of micro-sensors is crucial to realizing the full potential of microsystem components.

A functional sensor suitable for placement on metallic components must include an electrical insulation layer, a sensing layer, metallic interconnects, and a protective encapsulating layer. Thin film technology is the most promising means by which the necessary layers can be added to

microsystem components. This paper addresses the electrical strain response of directly deposited thin film sensing layers, the effects of encapsulation layers, and the effects resulting from ion irradiation.

Directly deposited thin film strain gages offer important advantages over conventional gages, including unobtrusive operation, negligible mass and profile, low current operation, and the potential for production in complex configurations with little added effort. In addition, the full range of processes and techniques of thin film science can be brought to bear for both manufacture and characterization of the resulting devices. Thus, structures can be tailored for specific applications, including, for example, layers of electrical or thermal insulation, while avoiding complex assembly steps involving delicate parts placement and adhesive application.

While direct deposition of metallic strain gages is possible, semiconductor materials have greater strain sensitivities while also being easily deposited in thin films. Although silicon is the most commonly used semiconductor material for strain sensing applications, processing issues make it undesirable for deposited gage applications. An alternative semiconductor material, indium-tin-oxide (ITO), has been

\* Corresponding author. Tel.: +1-615-343-6027; fax: +1-615-343-6614.  
E-mail address: [robert.a.weller@vanderbilt.edu](mailto:robert.a.weller@vanderbilt.edu) (R.A. Weller).



reported to exhibit large strain sensitivities [2,3] while also being readily prepared as a thin film by several processing techniques [4].

In this paper, we describe a novel two-step approach, combining pulsed laser deposition of ITO thin films and subsequent focused ion beam machining, to develop micro-scale sensors for micro-systems applications.

## 2. Background

The responsiveness of a strain-sensor is parameterized by a quantity called the gage factor,  $g$ , defined in Eq. (1) as the fractional resistance change per unit strain. In this equation,  $R$  is the initial resistance of the gage structure and  $\Delta R$  is the change in resistance accompanying a strain  $\varepsilon$ .

$$g \equiv \frac{\Delta R}{R} \frac{1}{\varepsilon} \quad (1)$$

For semiconductor gages, it is useful to elaborate upon Eq. (1) by separating the dependence of  $R$  on the geometry of the gage and the intrinsic resistivity  $\rho$  of the material used to make it. The result of this separation is Eq. (2), where Poisson's ratio  $\nu$  quantifies the contribution of geometric deformation to resistance change, and the effect the variation in intrinsic resistivity  $\Delta\rho/\rho$  is expressed explicitly.

$$g = 1 + 2\nu + \frac{\Delta\rho}{\rho} \frac{1}{\varepsilon} \quad (2)$$

The extrinsic geometric effects parameterized by  $\nu$  dominate in metal foil strain gages, and since most metals have  $\nu$  equal to 0.2–0.5, the gage factors for most metals are between 1.4 and 2. In semiconductor gages, geometric effects are minimal and often ignored. The variability of intrinsic resistivity with mechanical stress in an elastically strained material is called piezoresistivity [5].

Indium-tin-oxide (ITO) is known primarily as a transparent conductor and is the most widely used material with this unusual property [6]. ITO is almost always used commercially as a thin film and has been prepared in this form by evaporation, spray pyrolysis, magnetron sputtering, chemical vapor deposition, and pulsed laser deposition [4]. It is an n-type, degenerately doped, wide band gap semiconductor whose plasma frequency is just below the visible range of the spectrum and whose inter-band absorption edge is just above it. Charge carriers are thought to be provided by tin atoms in indium sites acting as donors and also by free electrons from oxygen vacancies.

ITO is used as a transparent electrode in such devices as organic light-emitting diodes [7], touch screen displays [8], flat panel displays [9], and lamps [4]. While ITO has been extensively studied to optimize electrical conductivity and transparency [10–12], it has only recently been reported to exhibit strain sensitivities characterized by gage factors reported in the range from  $-2$  to  $-77$  [2,3]. By comparison, the strain sensitivities of semiconductor silicon strain gages

are typically in the range 5 to 175 [13], while those of metal foil sensors are positive and typically in the range from about 2 up to approximately 6 [14]. The origin of piezoresistivity in crystalline semiconductors such as Ge and Si has been discussed by various authors [15]. However, in ITO the mechanism is unknown. Recently ITO has also been demonstrated to function as a sensor at high temperatures [16]. In [16], Gregory and Luo report the behavior of ITO strain gages prepared by magnetron sputtering and used together with temperature compensating platinum resistors to achieve a near zero temperature coefficient of resistance (TCR) over the range 25–1200 °C and operation up to 1450 °C.

Pulsed laser deposition (PLD) of ITO has several advantages over other thin film deposition techniques including the ability to control film stoichiometry through a combination of laser target stoichiometry and background pressure, and the ability to grow films at room temperature [4,10]. In addition, ITO is relatively impervious to deleterious effects of exposure to an oxygen environment, even at elevated temperatures. ITO solid solutions are stable in pure oxygen up to 1500 °C and do not undergo any disadvantageous phase transformations up to their decomposition temperature [16]. In this publication we confine the discussion to gage structures made by pulsed laser deposition and focus on issues related to making and characterizing gages as small as 20  $\mu\text{m} \times 100 \mu\text{m}$ .

## 3. Experiment details

ITO thin films were deposited by pulsed laser ablation. The laser target consisted of a pressed powder alloy of indium oxide (90%  $\text{In}_2\text{O}_3$ ) and tin oxide (10%  $\text{SnO}_2$ ), having a diameter of 7.6 cm at a distance of 4 cm from the substrate. A schematic of the apparatus is shown in Fig. 1. A krypton-fluoride excimer laser (Lambda Physik Compex 205) producing 248 nm pulses at 10 Hz with a 25 ns pulse duration and energy of 380 mJ/pulse yielded a fluence of  $\sim 0.13 \text{ J}/(\text{cm}^2 \text{ pulse})$ . Prior to all depositions the chamber was evacuated to a pressure of approximately  $6 \times 10^{-6}$  Torr and the target was cleaned with 5000 laser pulses.

Depositions for large-scale devices were performed at oxygen partial pressures ranging from 28 to 50 mTorr using 99.999% oxygen delivered by a mass flow controller. Small-scale devices were deposited at 50 mTorr, the highest achievable level in our system. The number of laser pulses was adjusted to produce film thicknesses in the range 100–300 nm.

Substrates were Corning glass 2935 with dimensions of 50 mm  $\times$  24 mm  $\times$  0.16 mm. Prior to deposition, substrates were cleaned in a series of sonic baths of acetone and methanol, rinsed in distilled water, and finally blown dry with compressed dry  $\text{N}_2$ . Film thicknesses were measured with a stylus profilometer (Dektak II).

The substrate containing the active gage element was strained in a four-point-bending configuration from 0 to 200

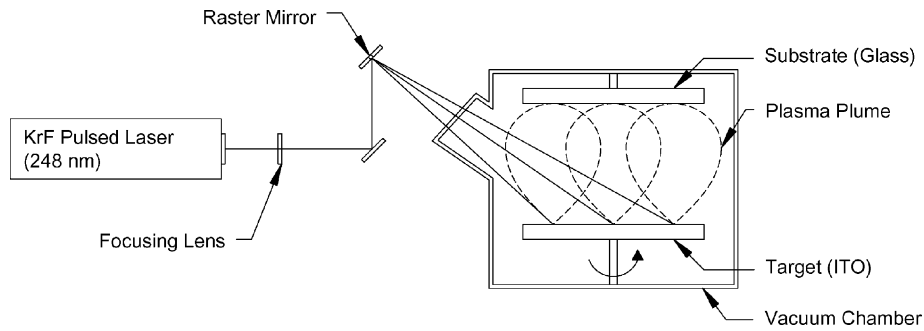


Fig. 1. Experimental set-up for pulsed laser deposition (PLD).

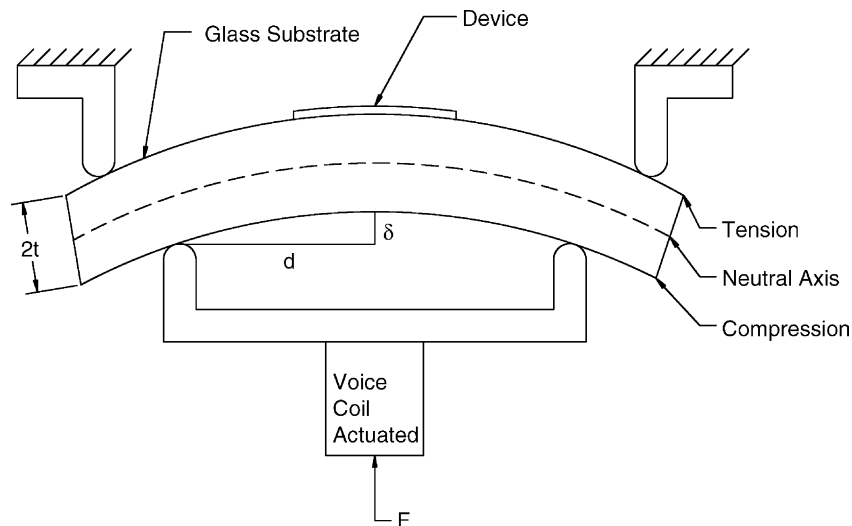


Fig. 2. Four-point bending apparatus used to induce a constant strain field in glass substrates between the inner pins. The device is actuated by a voice coil, which is driven by a precision digital power supply.

micro-strains (Fig. 2). This strain range is lower than that of some commercial gauges, but encompasses the full range anticipated to be important for the microsystems applications that originally motivated this work. A voice coil, powered by a digitally controlled constant current source (HP-E3631A) induced strain in the substrate. The strain may be calculated from simple geometry,  $\varepsilon = 2\delta t/(d^2 + \delta^2)$ , where  $t$  is the half-thickness of the substrate,  $\delta$  the deflection and  $2d$  is the inner pin spacing. The apparatus was calibrated using a commercial metal foil gage mounted conventionally with adhesives.

The gage patterns were designed for experimental determination of strain sensitivity by means of a four-wire resistance measurement (Fig. 3). They were formed using a 0.13 mm thick stainless steel shadow mask, shown in Fig. 4. Corresponding masks defined the locations for chromium metallization of the contact pads. Gage structures were designed to have an active area of  $790 \mu\text{m} \times 4.8 \text{ mm}$  for large-scale devices and  $250 \mu\text{m} \times 1.5 \text{ mm}$  for small-scale devices. Large-scale devices had  $2.38 \mu\text{m} \times 2.78 \text{ mm}$  contact pads while small-scale devices had  $760 \mu\text{m} \times 890 \mu\text{m}$  contact pads. Electrical contact was made using 25.4  $\mu\text{m}$  thick gold wire and H20E conductive epoxy from Epotek, Inc.

The 50–70 nm chromium adhesion layer deposited by thermal evaporation was used to improve electrical stability and contact resistance. The entire fixture was placed in a Faraday cage during  $I$ – $V$  characterization, which was performed using a Keithley 2001 7 1/2 digit multimeter for voltage measurement and a Keithley 236 constant current source.

The smallest gage structures were machined from larger ones using a model 200  $\times$ P focused ion beam from FEI, Co. Initially, gages were cut to  $100 \mu\text{m} \times 780 \mu\text{m}$ , and then scaled down to  $100 \mu\text{m} \times 400 \mu\text{m}$ , and finally  $20 \mu\text{m} \times 100 \mu\text{m}$ . Imaging and cutting operations with the focused ion beam (FIB) used 30 keV  $\text{Ga}^+$  ions at selectable current increments from 1 pA to 11.5 nA. Beam time and current were controlled during experiments to determine the radiation effects of imaging the ITO with the FIB. With the exception of focusing, imaging the ITO films in the FIB was typically done using a single raster scan of the area of interest at a beam current of 11, 70 or 150 pA. Cutting operations used currents of either 11.5 nA or 150 pA. Sections of ITO were electrically isolated by making open box cuts that overlapped the edges of the film. This method reduced etching time significantly as large areas of the active material did not have to be removed by sputtering, but were simply isolated from the

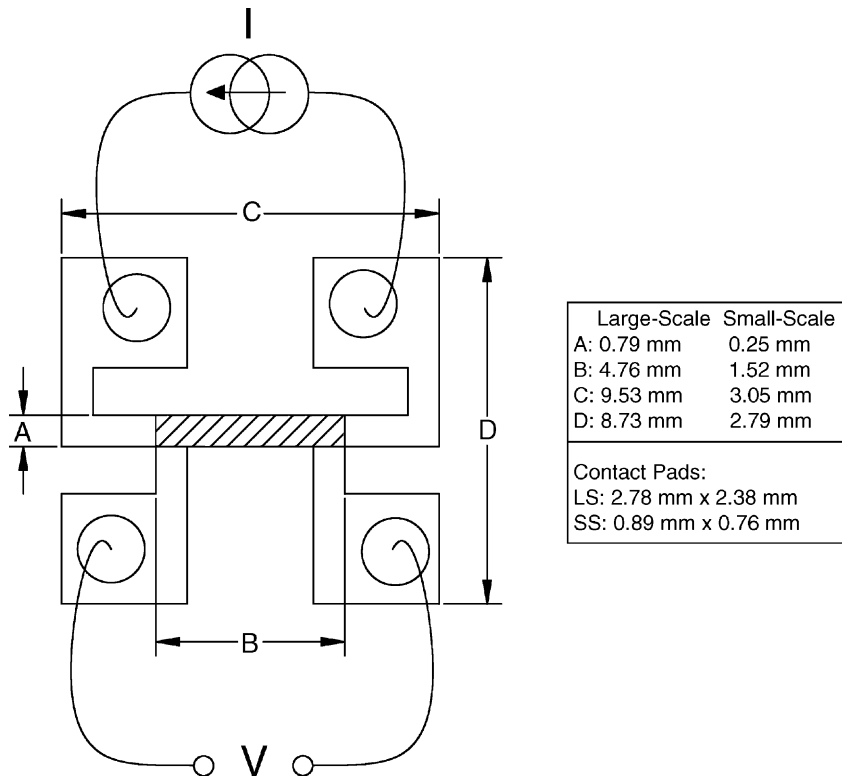


Fig. 3. Schematic of the test pattern used in electrical measurement showing the nominal dimensions for large- and small-scale gages. The central strip is aligned with the direction of axial strain in the four-point bend.

circuit electrically. Subsequent  $I$ - $V$  characterization and gage factor measurements were performed as outlined above.

Prior to FIB machining, an  $\text{SiO}_2$  encapsulation layer was deposited by PLD onto several ITO gages. The  $\text{SiO}_2$  layer was deposited using an SiO target and a background pressure of 40 mTorr of oxygen. This layer was deposited with a target-to-substrate distance of 6.5 cm, a height that required 1500 laser pulses to produce an  $\text{SiO}_2$  film  $\sim 100$  nm thick, or about 4 times the mean range of 30 keV  $\text{Ga}^+$  ions in  $\text{SiO}_2$ , a value

estimated to be 26 nm with range straggling of 6 nm. (Similarly, the range and straggling of 30 keV  $\text{Ga}^+$  in ITO are about  $13 \pm 6$  nm.) The thickness of the  $\text{SiO}_2$  layer was verified by ellipsometry using a Si substrate. After the ITO was encapsulated, the resistance and gage factor were re-measured.

#### 4. Results and discussion

Typically, the active gaging area for the films had a resistance of several thousand ohms. Large-scale gages had a range of resistance between 160  $\Omega$  and 600 k $\Omega$ , while small-scale gages had an average resistance of 55 k $\Omega$ . Commercial semiconductor strain gages typically have resistances of approximately 1 k $\Omega$ , while metal foil gages are either 120 or 350  $\Omega$ . Thus, ITO gages are potentially very attractive for low current, low power applications.

Fig. 5 shows gage factors and resistivities as a function of oxygen pressure during deposition for the large-scale devices, which were used in a series of experiments designed to optimize the strain sensitivity. Large-scale gages had a thickness ranging from 100 to 246 nm with an average standard deviation of 30 nm for three independent films deposited at a given pressure. Though not shown graphically, the thickness of these films did not show any apparent correlation with oxygen pressure. All gage factors were negative, though absolute values are plotted for convenience

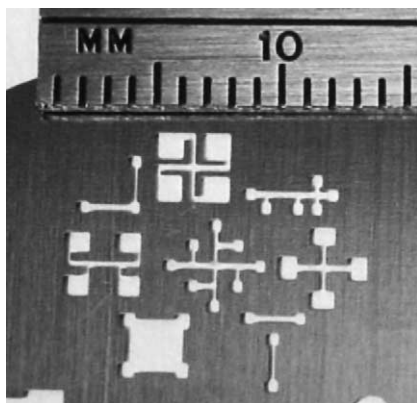


Fig. 4. A stainless steel shadow mask containing several small-scale gage patterns used to deposit thin film gage patterns. The four-point pattern center left is the gage structure used predominantly in this work.



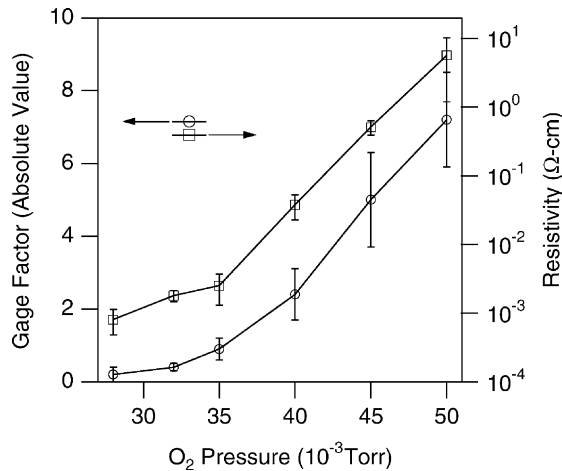


Fig. 5. Gage factor data (open circles) and resistivity data (open squares) plotted vs. oxygen partial pressure during deposition.

of representation. Each data point in the figure represents an average for three films made at the given pressure, with the error bars indicating one standard deviation.

The increase in resistivity with increasing oxygen pressure is consistent with previously published data and has been shown to be a critical parameter in determining the resistivity of ITO films [3,4,10]. Oxygen vacancies contribute charge carriers and as a result, varying the oxygen stoichiometry through oxygen background pressure during deposition is in effect a means for controlling carrier density. Fewer oxygen vacancies lead to fewer carriers and consequently higher resistivity, as shown by the data of Kim et al. [4]. Thus, the effect of the oxygen pressure on the strain sensitivity is of significant interest, although the precise mechanism for piezoresistivity has not been identified. In semiconductor Si gages and other materials with degenerate hole bands, strain breaks the degeneracy and leads to changes in the proportion of heavy and light holes as well as in the effective masses themselves. This is the reason that Si strain gages are consistently made of p-type material [15].

A dependence of gage factor on oxygen pressure during deposition similar to that of the resistivity was observed and is also shown in Fig. 5. It is important to emphasize that the well established oxygen pressure during deposition, which leads to maximum conductivity in ITO, approximately 10 mTorr, does not similarly maximize gage factor. In fact, for oxygen pressure values that maximize conductivity, the amplitude of the gage factor is at a minimum, with an average value of  $-0.2$ . When the oxygen pressure is increased to its maximum attainable level in our system, both the resistivity and the gage factor are maximized, with the gage factor having an average value of  $-7.2$ . Clearly, the oxygen pressure maintained during ITO deposition is a means of controlling both the conductivity and the strain sensitivity, although not independently.

The only other data available with which to compare the behavior of gage factor with oxygen partial pressure during deposition are those of Dyer et al. [2]. They found a gage

factor ranging between  $-11.4$  and  $-6.5$  for oxygen partial pressures in the range 1.2–4 mTorr. However, their data did not show a trend with pressure. In fact, it would be misleading to directly compare our data with theirs, because the residual atmosphere in their sputter system also contained Ar gas ranging from approximately 50–85%. The presence of Ar, which is used to improve sputtering yield, also substantially alters the energy distribution of the sputtered particles, which typically peaks at an energy of a few electronvolts. This, in turn, can have a decisive effect on the properties of a deposited thin film. In our system, the residual gas was composed entirely of oxygen. This gas both modified the velocity of the laser ablated material and reacted with it at the surface. Additional experiments are needed to separate the effects of these distinctly different physical processes.

As mentioned above, the sensitivity of the electrical properties of ITO to oxygen background pressure during deposition is well documented. However, the laser fluence was also found to have a significant effect on the electrical properties of the ITO films. In Fig. 6 the resistivity and gage factor of ITO films are plotted versus oxygen pressure for two different laser fluence levels. A clear shift can be seen in the curves for both resistivity and gage factor between data published previously (open circles) [3], and new data presented for the first time in this paper (open squares). The laser fluence previously was  $0.18 \text{ J/cm}^2$ , while for the current data it was  $0.13 \text{ J/cm}^2$ .

All small-scale gages were deposited exclusively in 50 mTorr of oxygen background pressure, and had an average gage factor of  $-4.0 \pm 0.8$ . The average thickness of nine films deposited with identical parameters was  $172 \pm 20 \text{ nm}$ . Fig. 7 shows a typical data set for a small-scale gage, in which the fractional change in resistance is shown as a function of applied strain. The sample shown has a resistance of 91 k $\Omega$

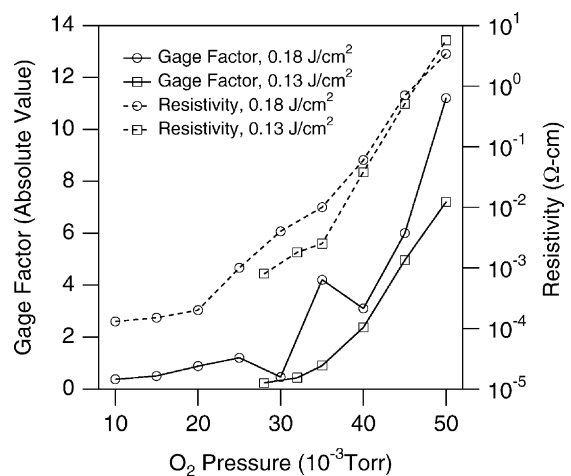


Fig. 6. This graph compares the curves of resistivity (dashed line), as well as gage factor (solid line), vs. oxygen pressure during deposition for two different laser fluence levels indicated in the legend. Previously published data from Fang et al. [3] (open circles) are shown together with new data (open squares).

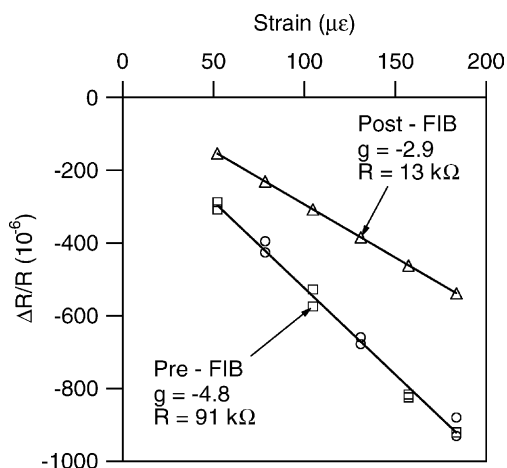


Fig. 7. The fractional change in resistance is shown plotted vs. strain for a small-scale gage (open circles and squares) and the subsequently FIB machined gage (open triangles). Results obtained during increasing strain (open circles) and decreasing strain (open squares) are shown separately to verify the absence of hysteresis.

and a gage factor of  $-4.8$ , as indicated by the slope of the curve. Error bars are not shown explicitly in the figure because the instrumental error for each point is less than 1%. The graph contains points measured during both increasing strain (circles) and decreasing strain (squares) for two distinct measurements and indicates a linear piezoresistive response as well as an absence of hysteresis that was typical of the films measured in this work.

Also shown in Fig. 7 is the piezoresistive response of the same sample after FIB machining to a size of  $100\ \mu\text{m} \times 780\ \mu\text{m}$ . The gage factor of the newly trimmed gage is smaller in magnitude than before, having a value of  $-2.9$ . However, the response is still linear and without hysteresis, as the data once again represent both increasing and decreasing strain cycles. The decrease in gage factor indicates collateral radiation damage during ion milling. The amount of FIB imaging of the full surface of this sample was minimal. However, the cuts were made using the largest available beam current, 11.5 nA, which also produces the largest and least well defined beam spot. What is more telling is that the resistance of this newly trimmed gage decreased by 86% to 13 k $\Omega$ . When altering the physical dimensions of a resistor, one expects a change in the resistance, but a decrease in resistance is unexpected, since the FIB cuts decreased the cross-sectional area. Evidently, electrical leakage paths were established either by imaging the gage area or by the beam halo in the regions adjacent to the FIB cuts.

In order to establish the location of the radiation damage affecting electrical properties, experiments were carried out with the goal of differentiating damage from imaging and that which resulted as a side effect of trimming the gage to net shape. An encapsulation layer of sufficient thickness should, in principle, protect a gage from surface damage, as well as minimize the effects of humidity and other environmental hazards. The SiO<sub>2</sub> encapsulation layer was deposited

Table 1  
A summary of the data from FIB imaging experiments

	Sample		
	1	2	3
Pre-FIB			
Resistance (k $\Omega$ )	2.3	280	3.8
G.F.	-2.5	-3.4	-2.4
Post-FIB			
Resistance (k $\Omega$ )	2.3	30	3.7
G.F.	-2.5	-2.4	-2.3
Processing			
nC/mm <sup>2</sup>	0.25	10.1	10.1
Beam current (pA)	11	150	150
Parameters			
Imaging	Minimal	Normal	Normal
Encapsulation	None	None	100 nm SiO <sub>2</sub>

onto the ITO layer by laser ablation of an SiO target in an oxygen ambient and experimentally verified to have no measurable effect on the electrical properties of the ITO. Both the resistance and the gage factor of several films remained the same as determined by  $I$ - $V$  measurements.

Table 1 summarizes a series of experiments to determine the effects of the radiation damage from FIB imaging on the electrical properties of ITO gages. Three samples were imaged with the FIB, two un-encapsulated samples at current and total dose levels differing by more than an order of magnitude, and the third, an encapsulated sample, subjected to the more intense exposure. The first sample was imaged several times using single scans at various scan rates and with a beam current of 11 pA. The total integrated current deposited on this sample, 329 pC in an area of approximately 1.3 mm<sup>2</sup>, did not produce any observable changes in the electrical properties of the ITO gage. The second sample was also imaged many times using single scans and different scan rates, but at a higher beam current of 150 pA. The total integrated beam current for this sample was approximately 13 nC in 1.3 mm<sup>2</sup>, and it produced a change in the resistance from 280 to 30 k $\Omega$ , and a reduction in the magnitude of the gage factor from 3.4 to 2.4. The third sample was encapsulated with 100 nm of SiO<sub>2</sub> and was imaged exactly as the second sample. The observed change, less than 3% in resistance and gage factor, proved that the SiO<sub>2</sub> effectively protects the ITO from the radiation damage accompanying imaging, at least for total fluences needed to set up, conduct, and verify ion machining operations.

Experiments were also performed to determine the effect that FIB milling has on the electrical properties of ITO gages. First, a cut was made in a sample parallel to the direction of current flow and in the center of the active gage element. The cut was made using the largest available beam current, 11.5 nA. The 5  $\mu\text{m}$  width of this cut was insignificant compared with the 300  $\mu\text{m}$  width of the full current path, and should not, therefore, have significantly affected the total resistance of the gage. Nevertheless, the operation

resulted in a 17% decrease in the gage resistance. To confirm the FIB's ability to cut through the ITO and effectively isolate parts of the current path, a second cut was made perpendicular to the direction of current flow and across the entire width of the gage. The result was as expected, a completely open circuit, effectively isolating the two halves of the gage.

Table 2 summarizes the results from three samples that were trimmed to different sizes using different beam currents. As the table indicates, directly machining un-encapsulated ITO reduced both the resistance and the absolute gage factors, even at a beam current of only 150 pA, where the size of the beam halo was substantially reduced. The situation with the encapsulated gage was more complex.

The encapsulated sample included 100 nm of SiO<sub>2</sub>, a layer sufficiently robust to protect the sensing layer from damage caused by imaging. This sample was trimmed to a size of 100 μm × 20 μm using a beam current of 150 pA. Prior to trimming, it had a resistance of 36 kΩ. After trimming to a smaller cross-sectional area, the resistance rose to 48 kΩ, a value that nevertheless fell short of the expectation based on geometrical considerations. However, the magnitude of the gage factor of this sample still decreased from a pre-irradiation value of -4.4 to a post-irradiation value of -3.6, indicating that despite the presence of the encapsulation layer, measurable radiation damage still occurred.

Table 2

A summary of the data from FIB machining experiments

	Sample		
	1	2	3
Pre-FIB			
Size (μm × μm)	1000 × 250	1000 × 250	1000 × 250
Resistance (kΩ)	91	89	36
G.F.	-4.8	-4.7	-4.4
Post-FIB			
Size (μm × μm)	780 × 100	400 × 80	100 × 20
Resistance (kΩ)	13	40	48
G.F.	-2.9	-2.8	-3.6
Processing parameters			
Cutting beam (pA)	11500	150	150
Encapsulation	None	None	100 nm SiO <sub>2</sub>

Collateral radiation damage near FIB cuts even at minimal beam currents and with encapsulated films is still sufficient to produce significant electrical effects. A FIB micrograph of this gage structure is shown in Fig. 8. Electrical isolation of the ITO above and below the narrow central active strip is seen to be total. These regions are dark as a result of a build-up of positive charge from the Ga<sup>+</sup> ion beam. This positive charge produces a voltage that suppresses secondary electrons, and results in the ITO in these regions appearing dark in the image. This is significant

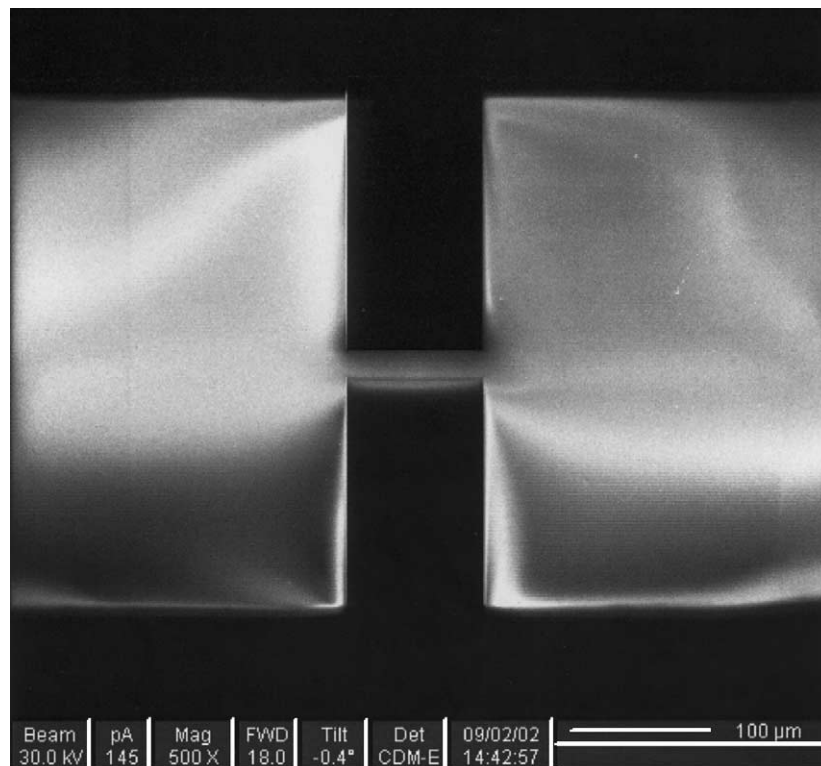


Fig. 8. An ion-induced secondary electron micrograph made in the FIB showing the 20 μm × 100 μm active area trimmed from the original deposited area, which was approximately 250 μm × 1000 μm. The dark regions above and below the strip still contain ITO but it is electrically separated from the sensor by a FIB cut, which extends into the substrate.

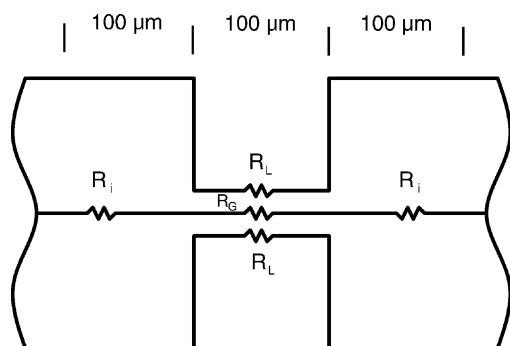


Fig. 9. A schematic that models the gage structure shown in Fig. 8. The leakage paths generated by radiation damage during trimming are modeled as resistors  $R_L$ . The undamaged gage material is assumed to have resistance  $R_G$ .

because it visually demonstrates that by selective narrow cuts the FIB has successfully trimmed the gage to size, effectively removing two large regions of ITO electrically without removing them physically.

To explore this effect quantitatively, a resistor model, shown in Fig. 9, was developed to estimate the resistance of the radiation damaged regions at the edges of the active area of the gage. This model, based on the results presented above, assumes that any change in the film's electrical properties results from trimming and not from imaging. Since the beam diameter is much less than a  $\mu\text{m}$ , one can assume that only a narrow region of ITO experiences a change in resistance as a result of alteration by the ion beam. Nevertheless, these current paths modeled as resistors  $R_L$  in Fig. 9 are effectively in parallel with the gage  $R_G$ , as shown schematically in the figure.

If one conceptually divides the original  $1000\ \mu\text{m}$  gage length into 10 segments of equal length, and assumes each segment is identical, then initially each segment has a resistance  $R_i$  of  $3.6\ \text{k}\Omega$ . Since the resistance of the entire gage after trimming was  $48\ \text{k}\Omega$ , the resistance of the trimmed segment with final width of  $20\ \mu\text{m}$  and length of  $100\ \mu\text{m}$  must be  $15.6\ \text{k}\Omega$ . With plausible assumptions about the film thickness profile, one can estimate the change in cross-sectional area resulting from the FIB cuts, and from this infer the resistance of the trimmed element, assuming no radiation damage. Using the three-resistors model in Fig. 9 one can then estimate the resistance of the areas damaged by the ion beam. Assuming a circular profile for the thickness of the original ITO gage, the resistance of the trimmed segment is estimated to increase from  $3.6$  to  $45\ \text{k}\Omega$ . This implies that the parallel resistors  $R_L$  modeling the leakage paths along the edges must have resistances of  $46\ \text{k}\Omega$  each in order to achieve the observed resistance of  $15.6\ \text{k}\Omega$ . If the thickness profile is instead assumed to be a rectangle bracketed by triangles, the resistance of the trimmed segment is estimated to increase to  $24\ \text{k}\Omega$ , implying that resistors  $R_L$  must have resistances of  $86\ \text{k}\Omega$ . Thus, we see that FIB machining produces leakage paths with resistance equivalent to  $50$ – $90\ \text{k}\Omega$ , with the exact value being dependent upon the thickness profile of the trimmed segment.

By applying similar reasoning, one can infer the gage factor of the trimmed element that would result in an overall change in the gage factor from  $-4.4$  to  $-3.6$ . Once again, one has to assume that each of the 10 hypothetical series segments has the same response to strain, and that only the trimmed segment is affected by the FIB. To carry out the analysis, one must account for the fact that when strained each uncut segment will undergo identical resistance changes  $\Delta R_i$ , while the machined segment will experience a unique resistance change  $\Delta R_G$ . By substituting  $(9\Delta R_i + \Delta R_G)$  for  $\Delta R$  in Eq. (1) and using the measured gage factor and resistance of the gage after the cut,  $\Delta R_G$  can be determined as a function of strain. Since the resistance of the trimmed segment is known to be  $15.6\ \text{k}\Omega$ , the gage factor of the  $20\ \mu\text{m} \times 100\ \mu\text{m}$  gage is estimated to be  $-2.0$ . Thus, as in other cases, radiation damage by the FIB decreases the gage factor of the ITO. However, it is important to note that the trimmed segment still has a gage factor comparable to that of metal foil gages.

## 5. Conclusion

Piezoresistive strain-sensors have been fabricated by combining pulsed laser deposition through masks onto room temperature substrates with focused ion beam machining to net shape. The active material, indium-tin-oxide, was fashioned reproducibly into sensors with high impedance, large gage factors, minimal hysteresis, and excellent linearity up to the 200 micro-strain limit of these measurements. For material deposited in a residual atmosphere of  $28$ – $50\ \text{mTorr}$  of oxygen, both resistivity and gage factor were found to increase in magnitude with increasing oxygen partial pressure. In addition, it was observed that laser fluence is a critical parameter in determining the piezoresistive properties of the films. However, the details of the mechanism for piezoresistivity in ITO have not been established.

The effect of radiation damage by the focused ion beam on the resistivity and gage factor of ITO was investigated. The generation of ion-induced secondary electron images resulted in minimal damage if done at low beam currents ( $11\ \text{pA}$ ) while larger beam currents ( $150\ \text{pA}$ – $11.5\ \text{nA}$ ) produced extensive collateral radiation damage when used for imaging or trimming a structure to net shape. Encapsulation of strain gages with a  $100\ \text{nm}$   $\text{SiO}_2$  layer produced no changes in the resistivities and gage factors, protected the ITO from ion beam damage during FIB imaging, and significantly reduced the radiation damage caused by trimming the gages to net shape.

## Acknowledgements

This work was supported by the US Army Research Office under Grant DAAD 19-99-1-0283 and by NASA,

Marshall Space Flight Center, under Graduate Student Researchers Program Grant NGT 8-52905.

## References

- [1] M. Goldfarb, N. Celanovic, A flexure-based gripper for small scale manipulation, *Robotica* 17 (1999) 181–187.
- [2] S.E. Dyer, O.J. Gregory, P.S. Amons, A. Bruins Slot, Preparation and piezoresistive properties of reactively sputtered indium tin oxide thin films, *Thin Solid Films* 288 (1996) 279–286.
- [3] H. Fang, T.M. Miller, R.H. Magruder II, R.A. Weller, The effect of strain on the resistivity of indium tin oxide films prepared by pulsed laser deposition, *J. Appl. Phys.* 91 (2002) 6194.
- [4] H. Kim, C.M. Gilmore, A. Piqué, J.S. Horwitz, H. Mattoussi, H. Murata, Z.H. Kafafi, D.B. Chrisey, Electrical, optical, and structural properties of indium-tin-oxide thin films for organic light-emitting devices, *J. Appl. Phys.* 86 (1999) 6451, and references therein.
- [5] C.S. Smith, Piezoresistive effect in germanium and silicon, *Phys. Rev.* 94 (1954) 42.
- [6] B.G. Lewis, D.C. Paine, Applications and processing of transparent conducting oxides, *MRS Bull.* 25 (2000) 22–27.
- [7] H. Kim, A. Piqué, J.S. Horwitz, H. Mattoussi, H. Murata, Z.H. Kafafi, D.B. Chrisey, Indium tin oxide thin films for organic light-emitting devices, *Appl. Phys. Lett.* 74 (1999) 3444.
- [8] M.J. Staines, Robust analog resistive touch-screen for computers, *Elektronik Praxis* no. 13 (2000) 44–47.
- [9] W.J. Lee, Y.K. Fang, J.J. Ho, C.Y. Chen, R.Y. Tsai, D. Huang, F.C. Ho, H.W. Chou, C.C. Chen, Pulsed-magnetron-sputtered low-temperature indium tin oxide films for flat-panel display applications, *J. Electron. Mater.* 31 (2002) 129.
- [10] Y. Wu, C.H.M. Marée, R.F. Haglund Jr, J.D. Hamilton, M.A. Morales Paliza, R.A. Weller, Resistivity and oxygen content of indium tin oxide films deposited at room temperature by pulsed-laser ablation, *J. Appl. Phys.* 86 (1999) 991.
- [11] H. Kim, J.S. Horwitz, G. Kushto, A. Piqué, Z.H. Kafafi, C.M. Gilmore, Effect of film thickness on the properties of indium tin oxide thin films, *J. Appl. Phys.* 88 (2000) 6021.
- [12] M.A. Morales Paliza, ITO, Indium Tin Oxide Films by Pulsed-Laser Ablation at Room Temperature, Ph.D. Dissertation, Vanderbilt University, 2001, and references therein.
- [13] L. Fang, W.L. Wang, P.D. Ding, K.J. Liao, J. Wang, Study on the piezoresistive effect of crystalline and polycrystalline diamond under uniaxial strains, *J. Appl. Phys.* 86 (1999) 5185–5193.
- [14] W.M. Murray, W.R. Miller, *The Bonded Electrical Resistance Strain Gage*, Oxford University Press, New York, 1992, pp. 13, 39.
- [15] P. Kleimann, B. Semmache, M. Le Berre, D. Barbier, Stress-dependent hole effective masses and piezoresistive properties of p-type monocrystalline and polycrystalline silicon, *Phys. Rev. B* 57 (1998) 8966–8971.
- [16] O.J. Gregory, Q. Luo, A self-compensated ceramic strain gage for use at elevated temperatures, *Sens. Actuators A* 88 (2001) 234–240.

## Biographies

*Timothy M. Miller* received an MS degree in materials science from Vanderbilt University in 2000. His thesis topic focused on phase transformations in titanium aluminides with ternary additions. He is currently completing an MS degree in mechanical engineering as a part of an interdisciplinary team working to develop thin film sensors for MEMS components.

*Hui Fang* is a PhD candidate in the Department of Physics and Astronomy at Vanderbilt University and is investigating the phenomenon of piezoresistivity in ITO thin films.

*Robert H. Magruder III* is a professor of physics at Belmont University with interests in the ion beam and pulsed laser deposition fabrication of thin films and optical characterization of thin films.

*Robert A. Weller* is an associate professor of electrical engineering at Vanderbilt, with interests in radiation effects in solids, ion beam fabrication and analysis of materials, electronic materials, and computer simulation of radiation effects in materials and devices.